Illumination: a new method for studying 3D percolation fronts in a concentration gradient

1992 J. Phys. A: Math. Gen. 25 3901

(http://iopscience.iop.org/0305-4470/25/14/010)

J. Phys. A: Math. Gen. 25 (1992) 3901-3912. Printed in the UK

Illumination: a new method for studying 3D percolation fronts in a concentration gradient

A Margolina† and M Rosso

Laboratoire de Physique de la Matière Condensée‡, Ecole Polytechnique, 91128 Palaiseau, France

Received 5 March 1992

Abstract. A new method of studying percolation fronts is introduced in situations where the concentration is not constant (gradient percolation approach): it consists in an efficient way of determining subsets of the percolation cluster which are exactly at the percolation threshold. The method is applied to both lattice and continuum percolation in order to determine the percolation threshold in 3D more accurately. Two variations of this method, illumination and projection, seem to give a similar scaling behaviour at low gradients for the cubic lattice case, leading to a new estimate for the percolation threshold: $p_c = 0.311\,73 \pm 0.000\,07$. For continuum percolation of overlapping spheres, the new estimate for the critical volume fraction is 0.291 ± 0.002, and the value of the critical exponent α_σ for the width of the front scaled with the concentration gradient is very close to the one for the lattice case.

1. Introduction

Gradient percolation approach [1-6] has proven to be a fruitful extension of the usual percolation problem. Percolation in a concentration gradient has been shown to be closely related to various physical problems including fractal interfaces in diffusion, corrosion, intercalation and invasion of porous media under gravity [7-9]. In addition, gradient percolation approach has provided a way to get the most precise estimates to date of the percolation for 2D lattice and continuum percolation [2, 4, 6].

Such an accurate determination of the percolation threshold p_c in 2D is based on the following observations. Due to the concentration gradient the infinite percolation cluster is limited by a front (external perimeter) whose structure is similar to that of a percolation cluster hull [10]. If the gradient is along a direction z, the front is restricted within a region where the average probability of occupied sites is equal to a value p_c^*, tending to p_c when the concentration gradient $\nabla p = \mathrm{d}p/\mathrm{d}z$ tends to 0 as

$$(p_c^* - p_c) \sim (\nabla p)^{\alpha_p} \tag{1}$$

where $\alpha_p \approx 1$ for the lattice [2] and continuum [6] cases in 2D. It is also of interest to study the width σ_f of the front which has been shown to scale as

$$\sigma_f \propto (\nabla p)^{-\alpha_\sigma} \tag{2}$$

where α_σ has been related to the exponent ν of the correlation length as $\alpha_\sigma = \nu/(1+\nu)$ and to the fractal dimension D_f of the front as $D_f = 1/\alpha_\sigma = (1+\nu)/\nu$ [1]. As $\nu = \frac{4}{3}$, in 2D, this gives $\alpha_\sigma = \frac{4}{7}$, and $D_f = \frac{7}{4}$, very close to both lattice [1] and continuum [6] simulations of gradient percolation in 2D. A considerable reduction of the computation

† Permanent address: Physics Department, Polytechnic University, 333 Jay Street, Brooklyn, NY11201, USA.
‡ Unité associée No 1254 du CNRS.

0305-4470/92/143901+12$04.50

time has been achieved due to the fact that the identification of the front is a relatively short procedure compared to the usual cluster recognition techniques in percolation problems.

However, in 3D the structure of the front has been found to be quite complex and its extension may be very wide [3, 5]. In the lattice case it extends through a probability region: $p_{c1} < p < 1 - p_{c2}$, where p_{c1} and p_{c2} are the percolation thresholds for the lattice of interest and its matching lattice [11]. The front has a fractal dimension $D_f \simeq 2.5$ close to p_{c1} or $1 - p_{c2}$, and is compact, with $D_f = 3$, in the region between them. In this sense the front may be considered as a representation for an ideally porous material [7]. Due to such an extension of the front its position no longer simply coincides with either of the thresholds p_{c1} or $1 - p_{c2}$. Moreover, we may expect that most of the front is not accessible [12]. Thus, the direct application of the gradient percolation approach to the 3D case, which is relevant to a number of experimental applications, does not yield a straightforward generalization of the successful 2D study. On the other hand, a more precise determination of the percolation threshold in the 3D lattice case and, especially, in the 3D continuum case, is of great value. For example, the best estimate to date for the percolation threshold of overlapping spheres [13] has not been improved for more than 15 years. At the same time, the recent applications of the continuum percolation using this result explicitly include the rubber-toughening of polymer blends [14, 15] and the conductivity of microemulsions [16]. The generalization of the gradient percolation to the 3D continuum case has bever been attempted and would be of great interest, especially in the case of polydispersity, where the results are very few.

In this paper we introduce a new method of studying the front in 3D which has allowed us to make an extension of the gradient percolation approach to 3D percolation. It consists in studying only the restricted parts of the front, which will be shown to be located at the percolation threshold $p_c = p_{c1}$. These parts could be viewed by *illuminating a percolation cluster from above* [17] *or by projection of the cluster* perpendicular to the concentration gradient. Hence, we shall consider two variations of this method, which may be compared to the sunlight shining on a cloud from above (at noon) or from the side (at sunset). In both cases we shall study the statistical distribution of the set formed by the most prominent features of the front. In the lattice case this method is straightforward and it leads to a new, more precise, estimate of p_c for a simple cubic lattice deduced from the average position of these illuminated subsets of the front. In the continuum case the application of the method is somewhat more complicated, and different ways of statistical analysis may be chosen. However, it yields a new, more precise estimate for p_c as well. The generalization to the case of polydispersity at this point is feasible.

The paper is arranged as follows. In section 2 we introduce the method with its two variations, namely the illumination and the projection methods, for both lattice and continuum cases. We also show that the illuminated and the projected parts of the front are at p_c. In section 3 we present our results for a simple cubic lattice and in section 4 we present those for a continuum percolation case. Our conclusions are presented in section 5.

2. *Illumination and projection of a percolation cluster at* p_c

Let us first consider the illumination method in a simple 3D lattice case. We define an illuminated site as a site which belongs to the percolating cluster with no other site

belonging to the percolating cluster in the lower p direction. In other words, if the concentration gradient is along the z-direction, with $p(z)$ decreasing while z increases, for each (x, y) in a plane perpendicular to z, the illuminated site is the site with the largest z which belongs to the percolating cluster. Such a site would be illuminated from a light source situated above it (in the low p/large z region). All the sites with the same (x, y) below the illuminated site would be in its shadow.

If $z_{max}(x, y)$ is the z-coordinate of an illuminated site then we define $p_{ci}^* = p(\langle z_{max} \rangle)$, where the average $\langle \ldots \rangle$ is taken over all (x, y) in a plane perpendicular to z. Identifying the illuminated sites is a straightforward operation for the computer (however, in contrast to the 2D case, where the front can be identified without identifying the entire percolating cluster, we still need here to determine the percolating cluster, and only then to find its illuminates sites). It remains to show that, in the limit of zero gradient, p_{ci}^* indeed tends to p_c. This follows since in this limit all illuminated sites tend to be at p_c. To see this, it is sufficient to consider the definition of the percolation probability $P_\infty(p)$ for the infinite cluster (the probability of a site to belong to the infinite cluster): it is zero below p_c, and larger than zero, increasing with p, above p_c. Thus, in a probability gradient the sites which are close to p_c may be divided into two groups: those below p_c tend not to belong to the infinite cluster, hence neither to its illuminated part. On the other hand, take a site S with coordinates (x, y, z_0), belonging to the infinite cluster, with $p(z_0) = p_0 > p_c$. If we make the gradient ∇p go to zero, the distance $z_0 - z_c$ between the site S and the site with coordinate z_c at which $p = p_c$, tends to infinity. As the probability $P_\infty(p)$ is positive for any $p > p_c$, this clearly means that the probability for the site S to be illuminated, i.e. the probability that there is no other site of the infinite cluster, with same x and y and $p_c < p < p_0$, tends to zero when $\nabla p \to 0$. In this way of thinking it is clearly seen that the illuminated sites (with highest z, still belonging to the infinite cluster) form a natural border or frontier between those two groups and, thus, tend to be at p_c.

In the projection method one makes a projection of a finite part of the infinite cluster on a plane parallel to z-direction. The low p front of this projection (with a definition similar to that of a 2D gradient percolation [1]) also tends to be at p_c. We then define $p_{cp}^* = p(z_{fp})$, where z_{fp} is the mean position of the projected front. In the next section, we shall see the results for both the illumination and the projection methods for a lattice case.

Both illumination and projection methods thus consist in recognizing subsets of sites, belonging to the infinite cluster, and situated in a region where p is as close as possible to p_c. This approach lies within the same framework of thinking as the concentration gradient method approach in 2D [1, 2].

The generalization of the illumination method to the continuum case is as follows. We consider the percolation of overlapping spheres of radius r_c, with a negative concentration gradient along the z-axis. Having identified the connected (infinite) cluster we find the illuminated spheres by imposing a square lattice with a certain mesh on a plane perpendicular to the gradient direction. At each node (x, y) of this lattice we identify the highest sphere belonging to the connected cluster. We call $z_{max}(x, y)$ the z-coordinate of the centre of this sphere. This sphere is then the illuminated sphere corresponding to a chosen mesh size (we have usually chosen a mesh size $r_c/2$ in our simulations). Of course, with a finer mesh size one may identify finer details of the illuminated part, which should result in a more accurate determination of the average position $\langle z_{max} \rangle$. Instead, one may use a finer statistics as another possibility to improve the precision, having observed that some spheres have spanned

several mesh sizes while the others (usually, the 'lower' ones) would only appear once or twice in overall statistics. Thus, there is a possibility to form a weighted average proportionally to the area which is illuminated for each sphere (this area is determined according to the mesh size). Namely, such a weighted average $\langle z_{max}\rangle_{wa}$ is given by $\Sigma_i n_i z_i/(\Sigma_i n_i)$, where n_i is the number of lattice nodes corresponding to a given sphere with a centre at z_i. We shall also calculate the usual average position $\langle z_{max}\rangle_{sa} = \Sigma_i z_i/N$, where N is the number of illuminated spheres.

Clearly, all the considerations for the average position of the illuminated of the front being at p_c apply also for a continuum case. The projection method may also be applied to the continuum case to find an alternative estimate of the percolation threshold. Both methods should also be applicable to polydisperse case.

3. Results for the simple cubic lattice

We have used $L' \times L' \times L$ lattices, where $L' = 176$ or $L' = 240$ and $L \leqslant 275$, with periodic boundary conditions in the x and y directions. The sites were coded using 2 bits as follows: 0—empty, 1—occupied, 2—connected. The occupation probability ranged from p_{min} to p_{max}, with $p_{min} < p_c < p_{max}$, so that the illuminated front has remained within these limits in all our samples. For the largest gradients one may take $p_{min} = 0$ and $p_{max} = 1$. Our gradients ranged from 1/50 to 1/4800. The occupation is decided according to a probability: $p(z) = p_{max} + (p_{min} - p_{max})z/L$. The recognition of an infinite cluster starts from p_{max} ($z = 1$): all occupied sites at $z = 1$ are considered connected, hence $P_\infty(p_{max}) = p_{max}$. This, obviously, introduces a systematic error, which is expected to disappear at z larger than the correlation length at p_{max}. The determination of the illuminated and the projected parts has been described above in detail, and these parts are shown in figures 1 and 2, respectively. It is interesting to note that the illuminated front is not necessarily connected and that, though its structure is still complex, it is visibly simpler than the whole 3D front of a percolation cluster.

The results of illumination and projection methods are shown in figures 3-5. Figure 3 shows how p^*_{ci} (illumination method) and p^*_{cp} (projection method) tend to p_c: from above for illumination, and from below for projection. We have verified that, at least for a lattice size L' much larger than the width σ_f of the illuminated front, the threshold p^*_{ci} does not depend on L'. On the other hand, the value of p^*_{cp} does depend on L' for the projection method (p^*_{cp} is larger for smaller L') in the whole investigated size range.

Assuming a scaling behaviour similar to equation (1) for both illuminated and projected fronts we write that p^*_{ci} and p^*_{cp} tend to p_c according to

$$(p^*_{ci} - p_c) \sim (\nabla p)^{\alpha_{pi}} \tag{3a}$$

$$(p^*_{cp} - p_c) \sim (\nabla p)^{\alpha_{pp}}. \tag{3b}$$

The fitting of our results to equation (3a) for *illumination* gives

$$p^*_{ci} = 0.311\,73 + 0.829 \times (\nabla p)^{0.725}$$

from which we obtain $p_c = 0.311\,73 \pm 7 \times 10^{-5}$, and $\alpha_{pi} = 0.725 \pm 0.004$. We wish to emphasize that the value for the threshold is rather sensitive to the value of α_{pi}. For example, $\alpha_{pi} = 0.72$ gives $p_c = 0.311\,65$, and $\alpha_{pi} = 0.73$ gives $p_c = 0.311\,82$. However the value we obtain for p_c with $\alpha_{pi} = 0.725$ remains within the error bar quoted above for a fit reduced to the n lower gradients shown in figure 4, with $n \geqslant 7$.

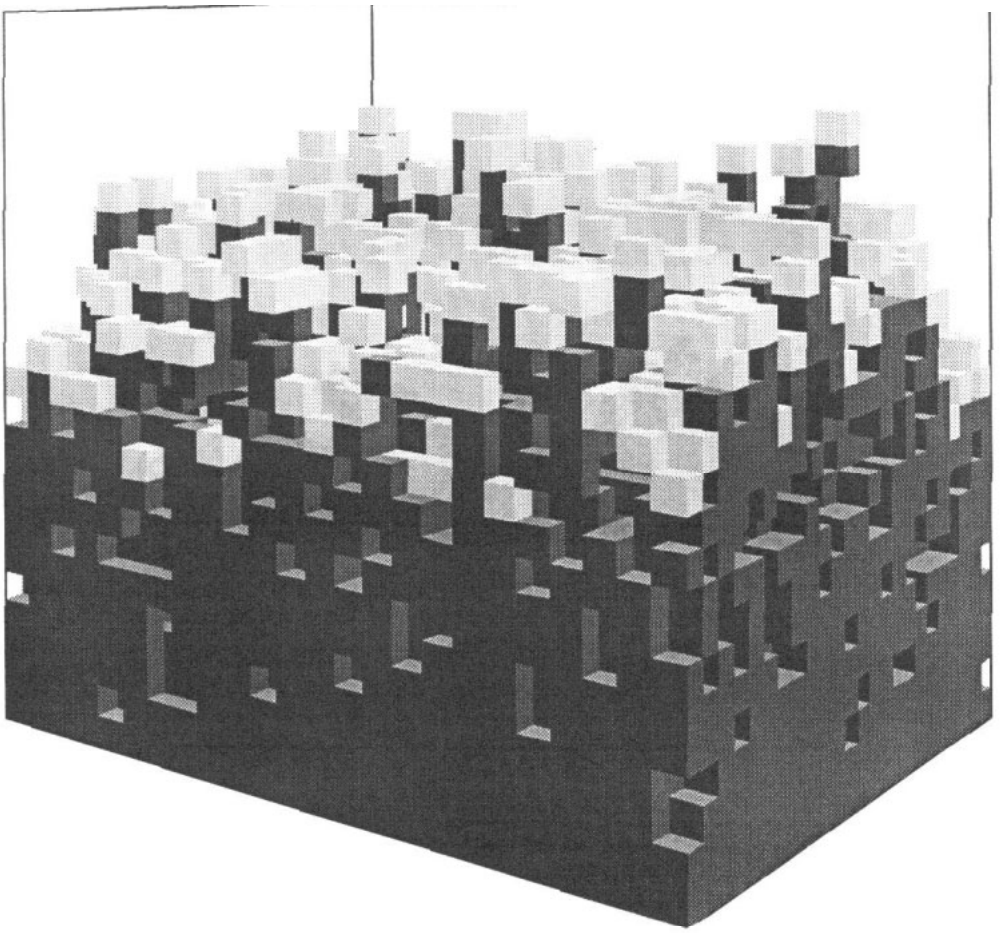

Figure 1. Illuminated front. In a $24 \times 24 \times 24$ simple cubic lattice, with concentration ranging from 0 to 1 from top to bottom, connected sites are shown as grey cubes: the illuminated sites (the highest in a given column) are shown in light grey.

The projection method has a slightly different scaling behaviour, at least for high gradients, as shown in figure 4. However, for low gradients, the two methods appear to have the same limiting behaviour, hence $\alpha_{pp} \simeq \alpha_{pi}$. Thus, both illuminated and projected parts of the 3D front seem to belong to the same universality class.

The new estimate of p_c needs to be compared with four most recent and accurate estimates: $p_c = 0.3117 \pm 0.0003$ [18], $p_c = 0.311\,605 \pm 10^{-5}$ [19], $p_c = 0.3116 \pm 0.0001$ [20], $p_c = 0.311\,58 \pm 0.000\,06$ [21] respectively. It is in agreement and more accurate than [18] and [20]. It is not in agreement with (somewhat higher than) [19]. It is compatible only with a higher estimate of [21]. The high accuracy of our results may be substantiated by the following comparison with the analysis made in [18]. As will be shown below, the width σ_{fi} of the illuminated front scales with the gradient according to equation (2), yielding $\alpha_{\sigma i} \simeq 0.436$. Thus, the width of the illuminated front in terms of the probability tends to zero as $w = \sigma_{fi} \times \nabla p \sim \nabla p^{0.564}$ when $\nabla p \to 0$ (whereas the width of the whole front in terms of the probability remains almost constant). Now $(p_{ci}^* - p_c)$

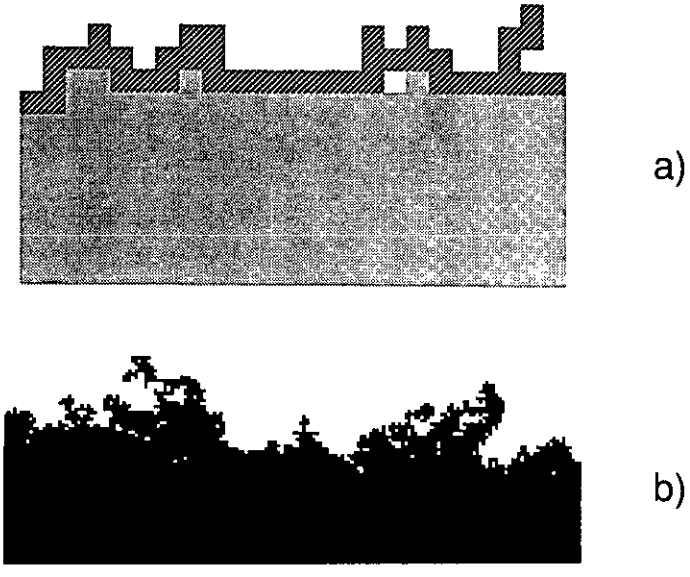

Figure 2. Projected fronts: (*a*) The connected cluster shown in figure 1 is represented here, as seen from the left. The low concentration front of this projection is shown as a hatched zone, at the top; (*b*) projection of the connected cluster, for a much smaller gradient ($\nabla p = 1/700$).

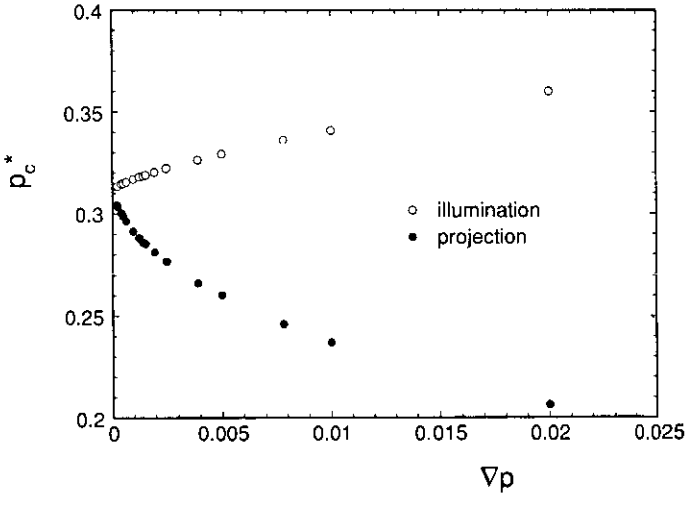

Figure 3. Variation of the average positions of illuminated and projected fronts as a function of the gradient ∇p.

converges to 0 as $\nabla p^{0.725}$, hence more rapidly than the width w. Thus it converges more rapidly than in the classical method [18], where the threshold for a given finite sample size L, $p_c(L)$ tends to p_c according to $p_c(L) - p_c \sim W$, where W is the uncertainty in $p_c(L)$, a parameter very close to our width w.

Finally, in figure 5 we present our results for the width of the illuminated and projected fronts. A generalization of equation (2) to the 3D case is straightforward,

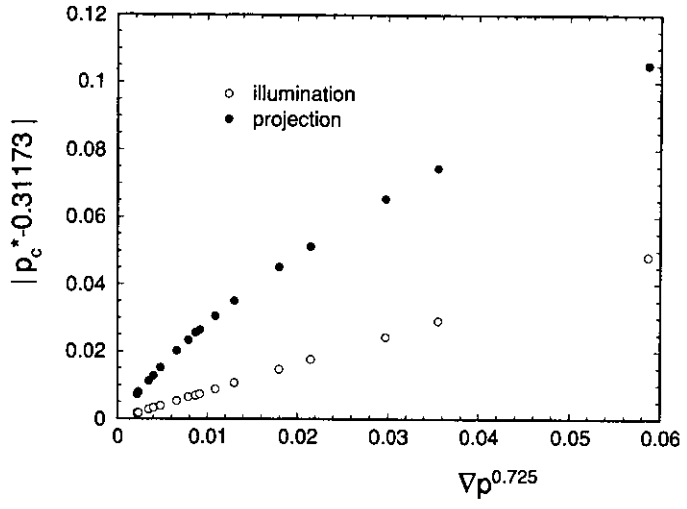

Figure 4. Variation of the average position of the projected front, scaled with $\nabla p^{0.725}$ (equations (4*a*), (4*b*)).

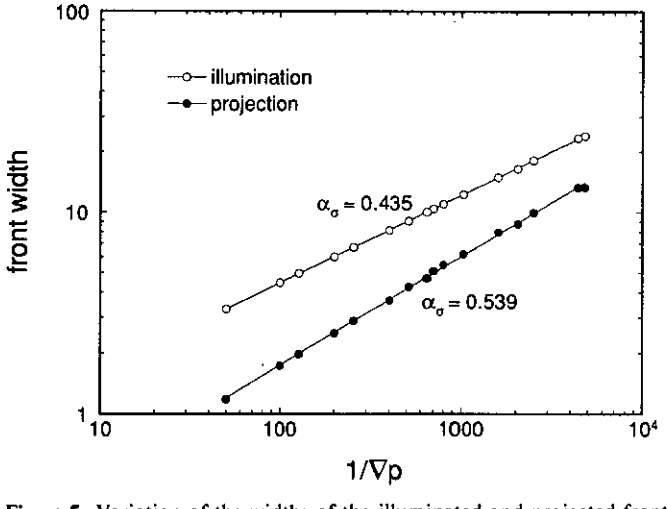

Figure 5. Variation of the widths of the illuminated and projected fronts as a function of the inverse gradients $1/\nabla p$.

assuming for the widths σ_{fi} (illumination) and σ_{fp} (projection) as a function of gradient the following scaling behaviour:

$$\sigma_{fi} \propto (\nabla p)^{-\alpha_{\sigma i}} \tag{4a}$$

$$\sigma_{fp} \propto (\nabla p)^{-\alpha_{\sigma p}}. \tag{4b}$$

Fitting our data to equation (4*a*, *b*) yields: $\alpha_{\sigma i} \approx 0.436$ for illumination, and a somewhat higher $\alpha_{\sigma p} \approx 0.539$ for projection. We note that both estimates are different from the expected value $\alpha_\sigma = \nu/(1+\nu) \approx 0.468$ for $\nu = 0.88$ in the 3D case. This could either be due to corrections to scaling or this could indicate some fundamental differences between the structures of the 2D front and the illuminated and projected fronts in 3D.

4. Results for continuum percolation

We have used a cubic box of size L^3, where L ranged from $30r_c$ to $140r_c$, with periodic boundary conditions in the x and y directions. The concentration of spheres $c(z)$ ranged from c_{min} at the top of the sample ($z = L$) to c_{max} at the bottom ($z = 0$), so that the critical concentration c_{crit} lies in this interval, and that the illuminated front remains within these limits for all our samples. The gradients ranged from $5.9 \times 10^{-4}\, r_c^{-4}$ to $7.1 \times 10^{-3}\, r_c^{-4}$. We identify the connected cluster starting from c_{max}, at which all spheres are considered connected (see above for the lattice case). The recognition of the illuminated part and the statistics of averaging is described above in detail. In the projection method a subset of the connected sites is considered, which lies in the low concentration region of the illuminated sites. For this reason, we could use this method for samples with narrower concentration distribution, hence smaller concentration gradients. In this case, the gradients have reached down to $2 \times 10^{-4}\, r_c^{-4}$.

Various equivalent definitions have been used in the literature for the percolation threshold of overlapping spheres [13, 22-29]. Following Kurkijärvi [24], we chose a definition for p_c which is independent from length units: $p_c = 4\pi/3\, c_{crit}\, r_c^3$. From this we shall determine the critical volume fraction (CVF), which is the fraction of the volume occupied by the overlapping spheres belonging to the percolating cluster to the overall volume: $\mathrm{CVF} = 1 - \exp(p_c)$.

The illuminated part is illustrated in figure 6. One can arrive in this case at the estimate of the percolation threshold following two different methods. First method:

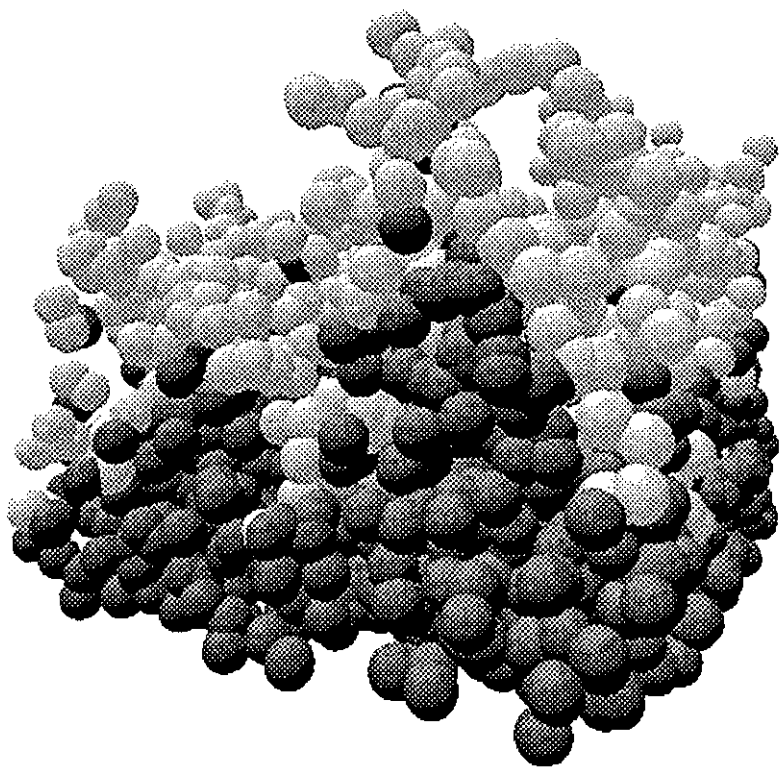

Figure 6. Illuminated part of the front in the continuum case. All connected spheres are shown: the connected, illuminated spheres are shown in light grey.

assume, due to universality, the same value $\alpha_{pi} \approx 0.725$ as in the lattice case and fit the data onto equation (3*a*). The results of this approach for both standard and weighted averages are shown on figure 7(*a*). The resulting estimate is $p_c \approx 0.341$ (standard average) or $p_c \approx 0.343$ (weighted average), with a somewhat better fit for the standard average. The second method requires a fit onto equation (3*a*) with no other assumption and the results are shown on figure 8. We obtain a somewhat higher value: $p_c \approx 0.344$ (standard average), with $\alpha_{pi} \approx 0.77$ or $p_c \approx 0.348$ (weighted average), with $\alpha_{pi} \approx 0.84$. Once more the fit is somewhat better for the standard average. Thus, our overall estimate for p_c is about 0.343 ± 0.002. The results are not as accurate as in the lattice case for two major reasons: the samples were much smaller here, while the smallest gradient we have considered is one order of magnitude larger than in the lattice case; the number of samples had to be reduced due to the increased time of computation.

Our general estimate for p_c corresponds to a critical volume fraction (CVF): CVF $\approx$ 0.291 ± 0.002. This result is well within the range of the most accepted values including

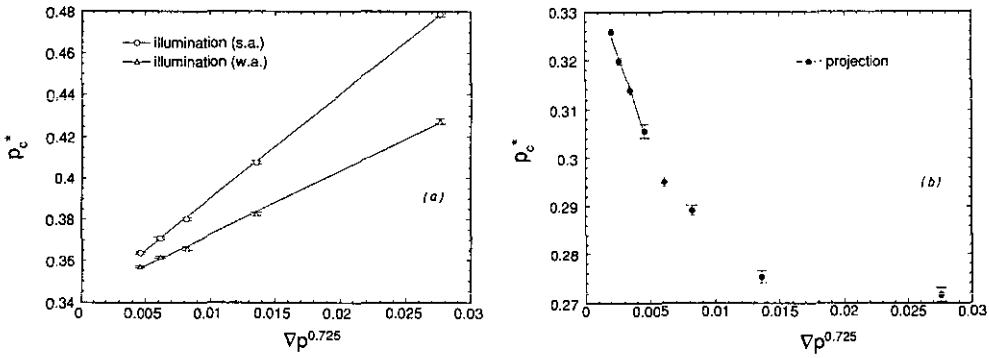

Figure 7. Variation of the average positions of the illuminated front, scaled with $\nabla p^{0.725}$: (*a*) illumination method, both for standard average and for weight average; (*b*) projection method. In this latter case the $(\nabla p)^{0.725}$ fit is performed on the four series of samples with smallest gradients and same size $L = 140\ r_c$.

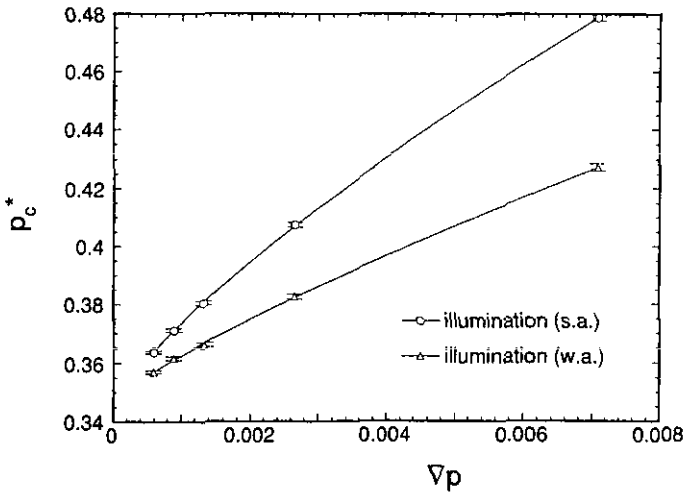

Figure 8. Best fits for the variation of the average positions of the illuminated front as a function of the gradient ∇p.

[13, 22–26]: CVF = 0.285 [13], CVF = 0.286 [22], CVF = 0.282 [23], CVF = 0.293 ± 0.008 [24], CVF = 0.286 ± 0.009 [25], CVF = 0.295 ± 0.018 [26], respectively. It is lower than CVF = 0.31 ± 0.006 [27], which may be considered as overestimated [13], and somewhat higher than CVF = 0.25 ± 0.02 [28]. As these results have not been verified for decades, our method seems to offer a possibility for such an improvement in precision.

The results of our study of the illumination front width σ_f are shown in figure 9. Both standard and weighted averages indicate values of α_σ very close to that for the lattice case: $\alpha_{\sigma isa} = 0.424$; $\alpha_{\sigma iwa} = 0.435$, while $\alpha_{\sigma i} = 0.436$ in the lattice case. Thus, the universality seems to be observed after all [29], which indicates favouring our first method of preserving $\alpha_{pi} = 0.725$ from the lattice case when seeking p_c. Thus a somewhat lower value of CVF ≈ 0.290 should be preferred.

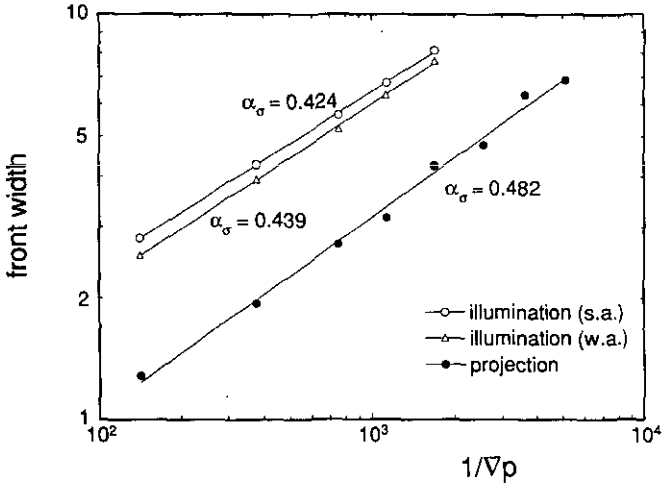

Figure 9. Variation of the width of the projected front as a function of the gradient ∇p, in illumination and projection methods.

Finally, the results for the projected front are shown in figures 7(*b*) and 9. The exponent for the width of the front is $\alpha_{\sigma p} = 0.48$: it is different from the exponent of the projected front in the lattice case (see previous section). We have no definite explanation for this fact at present. As in the lattice case, p^*_{cp} depends on the size L of the samples. Hence, to obtain the percolation threshold we made a fit on the results obtained for samples of the same size (see figure 7(*b*)). Using a $(\nabla p)^{0.725}$ fit, we obtain $p_c \approx 0.342$, a value very close to that obtained from the illumination method. Such an excellent correspondence is certainly very encouraging.

5. Discussion and conclusion

We have presented two different methods for studying the 3D percolation cluster in the framework of a gradient concentration approach. These two methods consist in an efficient way of determining subsets of the percolation cluster which are exactly at the percolation threshold. Following the gradient method derived in 2D, we use this approach to determine a better estimate of the percolation threshold in 3D.

Illuminated and projected fronts are shown to tend asymptotically to p_c as the gradient tends to zero: their average position is shown to converge to p_c according to equations (3*a*) and (3*b*). Within statistical errors, the exponents α_{pi} and α_{pp} are shown to be equal, and to apply in both lattice and continuum cases (universality).

The widths of the illuminated and projected fronts are found to scale (equations (4*a*), (4*b*)) with the concentration gradient. The exponents are slightly different for illumination and projection. In both cases they are different from the value which would be deduced from a generalization of the 2D front (equation (2)).

Illumination and projection methods may be compared as follows. The average position of the illuminated front is independent of the size of the sample, as long as this size is larger than the width σ_{fi}. On the other hand, the average position of the projected front does depend on the sample size. However we have found that, for a fixed sample size, the threshold p^*_{cp} determined from this position converges to p_c with the same exponent as p^*_{ci}, at least for small gradients.

In the continuum case, our generalization of the illumination method required the use of a mesh. We have checked the dependence of our results for p^*_{ci} as a function of the size of this mesh. The value p^*_{ci} (standard average) was found to depend on the mesh size, at least in the investigated range (mesh size of the order of the radius r_c). The use of a much smaller mesh size would have required much longer computer time. On the other hand, p^*_{ci} (weight average) was found to be almost independent of the mesh size in the same conditions. Note that, even though p^*_{ci} (standard average) does depend on the mesh size, we expect that its limit for zero gradient does not (this is due to the fact that, in the limit $\nabla p \to 0$, both the illuminated and the projected parts of the front tend to be at p_c, see section 2).

The projection method does not require the use of such a superimposed mesh; it requires slightly less computing time and permits the investigation of the gradient range to slightly smaller values. Hence, whereas in the lattice case the illumination method is preferable, for the continuum both methods may be used equally.

In conclusion, we have presented and analysed two new methods for studying the front of the percolation cluster in a concentration gradient. It has allowed us to achieve better estimates of the percolation thresholds for 3D lattice and continuum percolation. We have studied several scaling and universality features of the illuminated and projected fronts and compared them to those of standard percolation. Other 3D continuum percolation problems might also be investigated using these methods [30]. Their generalization to the case of polydisperse continuum percolation is underway.

Acknowledgments

We thank D Stauffer and J F Gouyet for useful comments and R Ziff for communicating to us his results before their publication. AM thanks Laboratoire de Physique de la Matière Condensée for its warm hospitality during the course of this study.

References

[1] Sapoval B, Rosso M and Gouyet J F 1985 *J. Physique Lett.* **46** 149
[2] Rosso M, Gouyet J F and Sapoval B 1985 *Phys. Rev.* B **32** 6053
[3] Rosso M, Sapoval B and Gouyet J F 1986 *Phys. Rev. Lett.* **57** 3195

[4] Ziff R and Sapoval B 1986 *J. Phys. A: Math. Gen.* **19** 1169
[5] Gouyet J F, Rosso M and Sapoval B 1988 *Phys. Rev.* B **37** 1832
[6] Rosso M 1989 *J. Phys. A: Math. Gen.* **22** L131
[7] Sapoval B, Rosso M and Gouyet J F 1989 *The Fractal Approach to Heterogeneous Chemistry* ed D Avnir (New York: Wiley)
[8] Hulin J P, Baudet C, Clement E, Gouyet J F and Rosso M 1988 *Phys. Rev. Lett.* **61** 333
[9] Gouyet J F, Rosso M and Sapoval B 1991 *Fractals and Disordered Systems* ed A Bunde and S Havlin (Berlin: Springer)
[10] Voss R F 1984 *J. Phys. A: Math. Gen.* **17** L373
[11] Essam J W 1972 *Phase Transitions and Critical Phenomena* ed C Domb and M Green (New York: Academic)
[12] Grossman T and Aharony A 1986 *J. Phys. A: Math. Gen.* **19** L745
Meakin P and Family F 1986 *Phys. Rev.* A **34** 2558
[13] Pike G E and Seager C H 1974 *Phys. Rev.* B **10** 1421
[14] Margolina A and Wu S 1988 *Polymer* **29** 2170; 1990 *Polymer* **31** 972
[15] Margolina A 1990 *Polymer Commun.* **31** 95
[16] Bug A L R, Safran S A, Grest G S and Webman I 1985 *Phys. Rev. Lett.* **55** 1896
[17] Mandelbrot B private communication
[18] Heermann D W and Stauffer D 1981 *Z. Phys.* B **44** 339
[19] Ziff R unpublished
[20] Gaunt D S and Sikes M F 1983 *J. Phys. A: Math. Gen.* **16** 783
[21] Wilkinson D and Barsony M 1984 *J. Phys. A: Math. Gen.* **17** L129
[22] Dalton N W, Domb C and Sikes M F 1964 *Proc. Phys. Soc.* **83** 496
Domb C and Dalton N W 1966 *Proc. Phys. Soc.* **89** 859
[23] Gayda J P and Ottavi H 1974 *J. Physique* **35** 393
[24] Kurkijärvi J 1974 *Phys. Rev.* B **9** 770
[25] Fremlin D H 1976 *J. Physique* **37** 813
[26] Hahn S W and Zwanzig R 1977 *J. Phys. A: Math. Gen.* **10** 1547
[27] Roberts F D K and Storey S H 1968 *Biometrika* **55** 258
[28] Holcomb D F and Rehr J J Jr 1969 *Phys. Rev.* **183** 773
[29] Gawlinsky E T and Stanley G E 1981 *J. Phys. A: Math. Gen.* **14** L291
[30] See for example Alon U, Balberg I and Drory A 1991 *Phys. Rev. Lett.* **55** 2879, and references therein